8564
NACA TN 2138

TECH LIBRARY KAFB, NM
0065069

NATIONAL ADVISORY COMMITTEE FOR AERONAUTICS

TECHNICAL NOTE 2138

ANALYTICAL AND EXPERIMENTAL INVESTIGATION OF ADIABATIC TURBULENT FLOW IN SMOOTH TUBES

By Robert G. Deissler

Lewis Flight Propulsion Laboratory
Cleveland, Ohio

Washington
July 1950

AFMDC
TECH LIBRARY
AFL 2811

RECEIVED HOLLOMAN AFB
ALAMOGORDO, N MEX
1950 JUL 31 AM 8:21

TECH LIBRARY KAFB, NM
0065069

NATIONAL ADVISORY COMMITTEE FOR AERONAUTICS

TECHNICAL NOTE 2138

ANALYTICAL AND EXPERIMENTAL INVESTIGATION OF ADIABATIC TURBULENT FLOW IN SMOOTH TUBES

By Robert G. Deissler

SUMMARY

Equations were derived for the prediction of velocity distributions for fully developed adiabatic turbulent flow in smooth tubes; both the incompressible- and compressible-flow cases were treated. The analysis produced a single equation that represents flow in both the conventional buffer layer and the laminar layer. By graphical integration of the velocity-distribution equations developed, a dimensionless flow-rate parameter was obtained and plotted. Use of the flow-rate parameter permits the prediction of pressure gradients along a tube for various flow rates.

In order to check the analysis and to determine values for the constants appearing in the equations, tests were conducted to determine velocity distributions in air flowing without heat transfer in a smooth tube having an inside diameter of 0.87 inch and a length of 87 inches. Data were obtained for fully developed velocity distributions and for developing velocity distributions at various distances from the entrance of the tube.

The results for fully developed flow were correlated by using conventional dimensionless velocity and distance parameters, and agreed closely with those of Nikuradse and other investigators. The plots of the equations and of the flow-rate parameter agreed well with the data when appropriate values of the two experimental constants appearing in the equations were used.

INTRODUCTION

Much empirical work has been done on the flow of fluids in tubes, and it has long been possible to predict fluid-flow pressure drops with a fair degree of accuracy by using experimentally determined friction factors (reference 1, pp. 232-272). Somewhat less work has been done in an effort to understand the mechanism of

turbulent flow in tubes and to develop a theory that is in complete agreement with the measurements. The Kármán similarity theory, which is perhaps the best-known contribution, satisfactorily predicts the velocity distributions for fully developed incompressible flow except in the vicinity of the wall (reference 2).

In an investigation made at the NACA Lewis laboratory, a new equation was developed that gives the relation between velocity and distance from the wall for both the laminar and the so-called buffer regions. For completeness, the Kármán-Prandtl development for the velocity distribution at a distance from a wall (turbulent region) is also included. In the present analysis, this development is extended to compressible flow, that is, to the case in which variation of temperature across the tube due to high velocities is appreciable.

Because of the scarcity of velocity-distribution data, especially for conditions under which compressibility might be appreciable, investigations were made to determine velocity distributions in a tube at various distances from the entrance and for fully developed flow. The results of these investigations, reported herein, are used to check the analysis.

ANALYSIS

General Turbulence Theory

During turbulent flow through a tube, portions of the fluid move about in random fashion. Inasmuch as a transverse-velocity gradient exists, some portions enter regions of various mean axial velocities. Momentum is then transferred from one portion to another and a shear stress, in addition to the viscous shear stress, is produced.

By analogy with the law for viscous shear stress $\tau_v = \mu\, du/dy$, the equation for the shear stress produced by turbulence is often given in the following form:

$$\tau_t = \rho\epsilon \frac{du}{dy} \tag{1}$$

where $\rho\epsilon$ is comparable to the viscosity for viscous shear μ, and ϵ is the coefficient of eddy diffusivity, the value for which

is determined by the amount and the kind of turbulent mixing at a point. (The symbols used in this report are defined in the appendix.)

1323

The analogy between shear stresses produced by viscosity and those produced by turbulence is not quite exact because the mechanism for momentum transfer is somewhat different for the two conditions. The chief difference probably is that in the case of viscous shear momentum transfer takes place suddenly at the instant the molecules collide; whereas in the case of turbulence, portions of the fluid can continuously transfer their momentum as they travel transversely inasmuch as they continuously act on one another. This difference can, however, be absorbed in the value of ϵ, which is descriptive of the turbulence mechanism, so that equation (1) should still be valid.

The total shear stress τ may be obtained by adding the viscous shear stress to the turbulent shear stress as follows:

$$\tau = \mu \frac{du}{dy} + \rho\epsilon \frac{du}{dy} \tag{2}$$

In order to make practical use of equation (2), ϵ must be evaluated for each portion of the flow. Because the actual mechanism of turbulent exchange of momentum is very complicated, the method of dimensional analysis is used and the constants obtained in the analysis are evaluated by experiment. From consideration of the various factors on which ϵ might depend, the following functional relation is assumed:

$$\epsilon = f\left(u, y, \frac{\mu}{\rho}, \frac{du}{dy}, \frac{d^2u}{dy^2}, \frac{d^3u}{dy^3}, \cdot \cdot \cdot\right)$$

Although the turbulence mechanism might conceivably depend on μ/ρ, the influence of this factor is assumed negligible and the validity of this assumption is experimentally checked.

Flow at a distance from wall. - It is shown by von Kármán (reference 2) that for flow at a distance y from a wall the shear stress is given by

$$\tau = \rho\kappa^2 \frac{\left(\frac{du}{dy}\right)^4}{\left(\frac{d^2u}{dy^2}\right)^2} \tag{3}$$

1323

where κ^2 is a constant of proportionality experimentally determined. Viscous shear stress is neglected in the derivation of this equation. Combination of this equation and equation (2), with the viscous shear stress neglected because it is small except in the region close to the wall, gives the following expression for local eddy diffusivity for flow at a distance from the wall:

$$\epsilon = \kappa^2 \frac{\left(\frac{du}{dy}\right)^3}{\left(\frac{d^2u}{dy^2}\right)^2} \tag{4}$$

Equation (4) could also have been obtained from the general functional relation for ϵ by assuming that only the first and second derivatives of the velocity with respect to distance are important in determining the value of ϵ, and by applying dimensional analysis. This fact indicates that the eddy diffusivity, or turbulent transfer of momentum, at a point away from the wall is chiefly dependent on the velocities in the vicinity of the point relative to the velocity at the point and is independent of the magnitudes of u and y. The fact that ϵ at a point away from the wall is dependent more on the velocity distribution than on the magnitude of the velocity u at the point may be illustrated by noting that at the smooth entrance to a tube, where the velocity profile is uniform over most of the cross section, turbulence at a point away from the wall is negligible compared with that farther down the tube at a point at which the mean axial velocity is equal to that at the entrance, but at which the flow profile is fully developed. This change from zero eddy diffusivity at the entrance to an appreciable degree of turbulence farther down the tube has been clearly shown by experiments with dye in a stream (reference 1, (Frontispiece.)). In the remainder of the analysis, equation (3) is used in calculating flow at points distant from the wall.

1323

Flow in vicinity of wall. - Although the effects of the magnitudes of u and y on ϵ can be neglected in considering flow at points distant from the wall, it appears that they must be accounted for in considering flow close to the wall. The experimental data available indicate that the turbulent transfer of momentum and thus the turbulent shear stress become very small in the region close to the wall, so that near the wall practically all shear stress is produced by viscous action and the velocity u is very nearly a linear function of y (reference 3). The second and possibly higher velocity derivatives therefore approach the constant value zero in the vicinity of the wall and the first derivative approaches a constant, which is defined when u and y are given. As previously stated, the effect of μ/ρ on ϵ is assumed negligible. As a first approximation, the functional relation for ϵ is therefore written as

$$\epsilon = f(u,y)$$

The range of values of y for which this approximation is sufficient will be experimentally determined. From dimensional analysis,

$$\epsilon = n^2 uy \tag{5}$$

where n^2 is a constant of proportionality to be determined experimentally. Substitution of equation (5) into equation (2) gives

$$\tau = \mu \frac{du}{dy} + n^2 \rho uy \frac{du}{dy} \tag{6}$$

In the remainder of the analysis, equation (6) is used in calculating velocity distributions close to the wall.

Equations for Incompressible Flow

Flow in vicinity of wall. - In order to obtain equations that are in dimensionless form, the following commonly used dimensionless quantities are employed: 1323

$$u^+ \equiv \frac{u}{\sqrt{\tau_0/\rho_0}} \tag{7}$$

$$y^+ \equiv \frac{\sqrt{\tau_0/\rho_0}}{\mu_0/\rho_0}\, y \tag{8}$$

Then

$$\frac{du}{dy} = \frac{\tau_0}{\mu_0}\frac{du^+}{dy^+} \tag{9}$$

and

$$\frac{d^2u}{dy^2} = \frac{\tau_0\sqrt{\tau_0/\rho_0}}{{\mu_0}^2/\rho_0}\frac{d^2u^+}{{dy^+}^2} \tag{10}$$

On substitution of equations (7) to (9), equation (6) becomes

$$\tau_0 = \mu_0\frac{\tau_0}{\mu_0}\frac{du^+}{dy^+} + n^2\cdot\rho_0\sqrt{\tau_0/\rho_0}\; u^+\frac{\mu_0}{\rho_0}\frac{y^+}{\sqrt{\tau_0/\rho_0}}\frac{\tau_0}{\mu_0}\frac{du^+}{dy^+}$$

where ρ and μ have been replaced by ρ_0 and μ_0, respectively, because the density and the viscosity are the same at all points for

incompressible flow. The shear stress τ has been approximated by τ_0 because only the region close to the wall is being considered and the variation in τ for this region is slight.

By rearrangement and cancellation of like terms, the preceding equation simplifies to

$$\frac{dy^+}{du^+} - n^2u^+y^+ = 1 \tag{11}$$

This equation is a first-order linear differential equation having the solution

$$y^+ = Ce^{\frac{(nu^+)^2}{2}} + e^{\frac{(nu^+)^2}{2}} \int_0^{u^+} e^{\frac{-(nu^+)^2}{2}} du^+$$

When $y^+ = 0$, then $u^+ = 0$ and

$$\int_0^{u^+} e^{\frac{-(nu^+)^2}{2}} du^+ = 0$$

Therefore $C = 0$ and

$$y^+ = e^{\frac{(nu^+)^2}{2}} \int_0^{u^+} e^{\frac{-(nu^+)^2}{2}} du^+$$

This equation can be rewritten as

$$y^+ = \frac{1}{n} \frac{\frac{1}{\sqrt{2\pi}} \int_0^{nu^+} e^{\frac{-(nu^+)^2}{2}} d(nu^+)}{\frac{1}{\sqrt{2\pi}} e^{\frac{-(nu^+)^2}{2}}} \tag{12}$$

where $\frac{1}{\sqrt{2\pi}} e^{\frac{-(nu^+)^2}{2}}$ is the normal error function of nu^+. (See reference 4.) The relation between u^+ and y^+ for incompressible flow near the wall is given in equation (12).

Flow at a distance from wall with shear stress uniform across the tube. - For flow at a distance from the wall, the analysis that was developed by von Kármán for the region near a wall (effect of viscosity neglected) and applied by Prandtl to the region at a distance from a wall is presented here. This application involves the assumption that the shear stress is constant across the tube, an assumption that will later be shown to be sufficiently accurate for this application. If this assumption is made and expressions (9) and (10) are substituted into equation (3),

$$\frac{d^2u^+}{dy^{+2}} = - \kappa \left(\frac{du^+}{dy^+}\right)^2 \tag{13}$$

This equation can be integrated to give

$$\frac{1}{\kappa} \frac{dy^+}{du^+} = y^+ + C_1$$

At the wall, the velocity gradient is very large compared with that at a distance from the wall so that dy^+/du^+ can be considered equal to zero when $y^+ = 0$, giving $C_1 = 0$ and

$$y^+ = \frac{1}{\kappa} \frac{dy^+}{du^+} \tag{14}$$

After the variables are separated, this equation can be integrated again to give

$$u^+ = \frac{1}{\kappa} \log_e y^+ + C \tag{15}$$

where C is a constant of integration, the value of which may be found when the ranges of applicability of the equations for flow close to a wall and at a distance from a wall are known. The ranges of applicability for the equations are to be experimentally determined. The relation between u^+ and y^+ for incompressible flow at a distance from the wall when constant shear stress across the tube is assumed is given in equation (15).

Flow at distance from wall with variable shear stress across the tube. - A result that avoids the assumption of uniformity of shear stress across the tube was derived by von Kármán substantially as follows: The relation for the variation of shear stress with radius for fully developed flow is obtained by equating the shear forces to the pressure forces acting on a cylinder of fluid of arbitrary radius and differential length (reference 5). This relation is

$$\tau = \frac{r}{r_0} \tau_0 = \left(1 - \frac{y}{r_0}\right) \tau_0$$

or

$$\tau = \left(1 - \frac{y^+}{r_0^+}\right) \tau_0 \tag{16}$$

where

$$r_0^+ = \frac{\sqrt{\tau_0/\rho_0}}{\mu_0/\rho_0} r_0 \tag{17}$$

On substitution of equations (7) to (10) and (16), equation (3) becomes, in dimensionless form,

$$\sqrt{1 - \frac{y^+}{r_0^+}} = - \kappa \frac{\left(\frac{du^+}{dy^+}\right)^2}{\frac{d^2u^+}{dy^{+2}}} \tag{18}$$

where the negative sign was selected on taking the square root in order to make κ positive.

The first integration gives

$$\frac{dy^+}{du^+} = - 2\kappa \sqrt{r_0^+} \sqrt{r_0^+ - y^+} + C_1$$

As previously stated, the velocity gradient at the wall is very large compared with that at a distance from the wall and dy^+/du^+ can be considered to be zero at the wall (that is, at $y^+ = 0$). Hence

$$C_1 = 2\kappa r_0^+$$

and

$$\frac{dy^+}{du^+} = - 2\kappa \sqrt{r_0^+} \sqrt{r_0^+ - y^+} + 2\kappa r_0^+ \tag{19}$$

1323

By substitution of $X^2 = r_0^+ - y^+$, equation (19) can be integrated to give

$$u^+ = \frac{1}{\kappa}\left[\sqrt{1 - \frac{y^+}{r_0^+}} + \log_e\left(1 - \sqrt{1 - \frac{y^+}{r_0^+}}\right)\right] + C \tag{20}$$

Equation (20), which is substantially the equation obtained by von Kármán, relates u^+ to y^+ for various values of r_0^+. Taking the variation of shear stress into account introduces the additional dimensionless parameter r_0^+, which will be called the tube-radius parameter. The equations developed by von Kármán for the flow distant from the wall will be extended for compressible flow by a method subsequently developed herein.

Equations for Compressible Flow

In the derivation of the compressible-flow equations, uniformity of shear stress across the tube is assumed and the error introduced is discussed in the section "Effect of Variable Shear Stress."

Flow in vicinity of wall. - For compressible flow in a tube, the static temperature and thus the density and the viscosity vary across the tube. For flow without external heat transfer, the total temperature at any point across the tube is practically the same as the wall temperature, so that the static temperature is given by

$$t = T_0 - \frac{u^2}{2gJc_p} \tag{21}$$

This relation is exact for a Prandtl number of 1.

By use of the perfect gas law, the density ρ may be expressed as

$$\rho = \frac{p}{gRt} = \frac{p}{gR\left(T_0 - \frac{u^2}{2gJc_p}\right)} = \frac{p}{gRT_0\left(1 - \frac{u^2}{2gJc_pT_0}\right)}$$

or

$$\rho = \frac{\rho_0}{1 - \frac{u^2}{2gJc_pT_0}} \tag{22}$$

1323

where the static pressure p has been assumed uniform across the tube.

Viscosity is a function of temperature and can be represented by an equation of the form

$$\mu = Kt^d \tag{23}$$

where K is some constant. Then

$$\mu = K\left(T_0 - \frac{u^2}{2gJc_p}\right)^d = KT_0{}^d\left(1 - \frac{u^2}{2gJc_pT_0}\right)^d$$

or

$$\mu = \mu_0\left(1 - \frac{u^2}{2gJc_pT_0}\right)^d \tag{24}$$

Substituting these values for the density and the viscosity into equation (6) and letting $\tau = \tau_0$ result in

$$\tau_0 = \mu_0\left(1 - \frac{u^2}{2gJc_pT_0}\right)^d \frac{du}{dy} + \frac{\rho_0}{1 - \frac{u^2}{2gJc_pT_0}} n^2uy\frac{du}{dy} \tag{25}$$

1323

Substituting values from equations (7) to (9) into equation (25), in order to convert it to a dimensionless form, gives

$$\frac{n^2u^+y^+}{1-\alpha u^{+2}}\frac{du^+}{dy^+} + \left(1 - \alpha u^{+2}\right)^d \frac{du^+}{dy^+} = 1 \tag{26}$$

where

$$\alpha \equiv \frac{\tau_0}{2gJc_pT_0\rho_0} \tag{27}$$

The dimensionless parameter α will be called the compressibility parameter. After rearrangement, equation (26) becomes

$$\frac{dy^+}{du^+} - \frac{n^2u^+}{1 - \alpha u^{+2}}\, y^+ = \left(1 - \alpha u^{+2}\right)^d \tag{28}$$

which is a first-order linear differential equation with variable coefficients. Solving equation (28) and setting the constant of integration equal to zero, as was done in the solution of equation (11), gives

$$y^+ = \left(1 - \alpha u^{+2}\right)^{\frac{-n^2}{2\alpha}} \int_0^{u^+} \left(1 - \alpha u^{+2}\right)^{\frac{n^2}{2\alpha} + d} du^+ \tag{29}$$

For compressible flow in the vicinity of the wall, equation (29) gives the relation between u^+ and y^+ for various values of α.

Flow at a distance from wall. - With the assumption of uniform shear stress, equation (3) can be written for compressible flow as

$$\tau_0 = \frac{\rho_0}{1 - \frac{u^2}{2gJc_pT_0}} \kappa^2 \frac{\left(\frac{du}{dy}\right)^4}{\left(\frac{d^2u}{dy^2}\right)^2}$$

1323

When written in dimensionless form, this equation becomes

$$\frac{d^2u^+}{dy^{+2}} = -\frac{\kappa}{\sqrt{1 - \alpha u^{+2}}}\left(\frac{du^+}{dy^+}\right)^2 \tag{30}$$

One integration of equation (30) can be made by substituting $v = du^+/dy^+$ and $dy^+ = du^+/v$ and then separating the variables. After one integration, equation (30) becomes

$$\log_e\left(C_1 \frac{du^+}{dy^+}\right) = -\frac{\kappa}{\sqrt{\alpha}} \sin^{-1}\left(\sqrt{\alpha}u^+\right)$$

or

$$C_1 \frac{du^+}{dy^+} = e^{-\frac{\kappa}{\sqrt{\alpha}} \sin^{-1}\left(\sqrt{\alpha}u^+\right)} \tag{31}$$

or

$$dy^+ = C_1 e^{\frac{\kappa}{\sqrt{\alpha}} \sin^{-1}\left(\sqrt{\alpha}u^+\right)} du^+ \tag{32}$$

If $\frac{\kappa}{\sqrt{\alpha}} \sin^{-1}\left(\sqrt{\alpha}u^+\right)$ is set equal to Z, equation (32) can be integrated to yield

$$y^+ = \frac{C_1}{\kappa^2+\alpha}\left[e^{\frac{\kappa}{\sqrt{\alpha}}\sin^{-1}(\sqrt{\alpha}u^+)}\right]\left(\kappa\sqrt{1-\alpha u^{+2}}+\alpha u^+\right)+C$$

By substituting dy^+/du^+ from equation (31) for $C_1 e^{\frac{\kappa}{\sqrt{\alpha}}\sin^{-1}(\sqrt{\alpha}u^+)}$ in the immediately preceding equation and letting dy^+/du^+ equal zero when y^+ and u^+ equal zero, C equals zero and thus

$$y^+ = \frac{C_1}{\kappa^2+\alpha}\left[e^{\frac{\kappa}{\sqrt{\alpha}}\sin^{-1}(\sqrt{\alpha}u^+)}\right]\left(\kappa\sqrt{1-\alpha u^{+2}}+\alpha u^+\right) \tag{33}$$

For compressible flow at a distance from the wall, equation (33) shows the relation between u^+ and y^+ for various values of α.

Summary of Velocity-Distribution Equations

The important equations that have been derived are assembled here for convenience:

For incompressible flow close to the wall,

$$y^+ = \frac{1}{n}\,\frac{\frac{1}{\sqrt{2\pi}}\int_0^{nu^+} e^{\frac{-(nu^+)^2}{2}}\,d(nu^+)}{\frac{1}{\sqrt{2\pi}}\,e^{\frac{-(nu^+)^2}{2}}} \tag{12}$$

where $\frac{1}{\sqrt{2\pi}}\,e^{\frac{-(nu^+)^2}{2}}$ is the normal error function of nu^+.

For incompressible flow at a distance from the wall, with shear stress uniform across the tube,

$$u^+ = \frac{1}{\kappa} \log_e y^+ + C \tag{15}$$

For incompressible flow at a distance from the wall with shear stress variable across the tube,

$$u^+ = \frac{1}{\kappa}\left[\sqrt{1 - \frac{y^+}{r_0^+}} + \log_e \left(1 - \sqrt{1 - \frac{y^+}{r_0^+}}\right)\right] + C \tag{20}$$

For compressible flow close to the wall,

$$y^+ = \left(1 - \alpha u^{+2}\right)^{\frac{-n^2}{2\alpha}} \int_0^{u^+} \left(1 - \alpha u^{+2}\right)^{\frac{n^2}{2\alpha} + d} du^+ \tag{29}$$

For compressible flow at a distance from the wall with shear stress uniform across the tube,

$$y^+ = \frac{C_1}{\kappa^2 + \alpha}\left[e^{\frac{\kappa}{\sqrt{\alpha}} \sin^{-1} (\sqrt{\alpha} u^+)}\right]\left(\kappa \sqrt{1 - \alpha u^{+2}} + \alpha u^+\right) \tag{33}$$

APPARATUS

A schematic diagram of the experimental apparatus used is shown in figure 1. Air at a pressure of about 40 pounds per square inch gage and at approximately room temperature flowed through two control valves in parallel, then through a filter, an orifice, a calming tank, a test section, and into the atmosphere.

Test section. - The test section consisted of a smooth Inconel tube having an inside diameter of 0.87 inch, an outside diameter of 1.0 inch, and a length of 87 inches. The calming tank was so constructed that either a rounded or a right-angle-edge entrance to the tube could be used; the rounded entrance consisted of a standard A.S.M.E. long-radius nozzle. Static pressures were measured through 0.03-inch holes drilled in the tube at the positions shown in figure 1. Air total temperatures were measured by thermocouples located at the inlet and outlet of the tube; these measurements provided a check on whether heat transfer took place through the tube wall.

Total-pressure measurements. - Openings for taking total-pressure measurements across the tube were located as shown in figure 1. Holes having 0.15-inch diameters through which a total-pressure probe entered the tube were drilled in the tube wall. These holes were located at right angles to the static-pressure taps. A probe actuator to move the probe across the tube and to measure its distance into the tube was fitted into a short length of tubing at each opening. The location of the total-pressure probe with respect to the opening in the tube is shown in the insert in figure 1. The total-pressure probe used for the measurements had a 0.016-inch-diameter opening and a 0.002-inch wall at the tip. The probe was flattened out for some of the runs so that the width of the opening was 0.005 inch. The probe was made so that the tip just cleared the edge of the 0.15-inch hole in the test section. The total projected area of the probe in the direction of flow with the tip at the center of the tube was about $1\frac{1}{2}$ percent of the area of the tube, but the effective blocking area at the tip was considerably less because the main portion of the probe was downstream of the tip.

METHODS

Procedure

In order to establish the applicability of the equations derived for fully developed flow, velocity distributions at various distances from the tube entrance were first determined. Measurements were made at Reynolds numbers of approximately 40,000, 160,000, and 580,000 with both rounded and right-angle-edge entrances and with corresponding tube-exit Mach numbers up to 1. The flow rate in each case was obtained by adjusting the inlet pressure.

A more extensive series of investigations was then conducted to determine velocity distributions for fully developed flow including distributions for the region close to the wall. Runs were made at about 20 different Reynolds numbers between 10,000 and 200,000 and with Mach numbers up to 0.5 with the total-pressure probe near the exit of the tube where the flow was practically fully developed. Runs were made with both the rounded and the right-angle-edge entrances. Total-pressure readings were taken at points between the wall in which the probe opening was located and the center of the tube. Readings near the opposite wall were inaccurate because of disturbance due to the probe.

Measurements were made with both the round and the flattened probe tips in order to determine whether presence of the probe had any effect on the measured velocity distributions in the vicinity of the wall. Because no appreciable difference could be noticed between the measurements made with the two types of tip, it was concluded that the presence of the probe did not affect the measurements and that the aerodynamic and geometric centers of the hole coincide.

Preliminary runs at high and at low flow rates showed that the total temperature of the air was uniform along the length of the tube, indicating that no heat transfer occurred. The air total temperature was therefore measured only at the outlet.

The following quantities were measured for each run: air flow, static pressures at the wall, air total temperature, total pressure at various positions across the tube, and distance of the probe tip from the wall.

Reduction of Experimental Data

Velocities. - For low air-flow rates, incompressible-flow theory was used; the velocities were calculated from the equation

$$P - p = \frac{1}{2} \rho u^2$$

where ρ was found from the equation of state for perfect gases

$$p = \rho g R t$$

1323

and t was taken equal to the total temperature. In this and in all succeeding calculations, the static pressure was assumed to be uniform across the tube.

For Mach numbers greater than 0.2, velocities were calculated from the relation

$$\frac{P}{p} = \left(1 + \frac{\gamma-1}{\gamma}\frac{u^2}{2gRt}\right)^{\frac{\gamma}{\gamma-1}}$$

where $t = T\left(\frac{p}{P}\right)^{\frac{\gamma-1}{\gamma}}$

Shear stress. - The shear stress at the wall for fully developed flow is related to the friction-pressure gradient by the equation

$$\tau_0 = -\frac{D}{4}\left(\frac{dp}{dx}\right)_{fr}$$

The friction-pressure gradients were obtained by subtracting calculated momentum-pressure gradients from the measured static-pressure gradients along the tube; the momentum-pressure gradients were calculated from

$$\left(\frac{dp}{dx}\right)_{mom} = \frac{w^2}{\rho_b{}^2A^2g^2}\frac{d\rho_b}{dx}$$

where ρ_b was found from the equation of state

$$p = \rho_b gRt_b$$

and

$$t_b = \frac{-1 + \sqrt{1 + 2\,\dfrac{w^2R^2T}{gJc_pA^2p^2}}}{\dfrac{w^2R^2}{gJc_pA^2p^2}}$$

1323

The last equation was obtained from the equations of energy, continuity, and state. The pressure and density gradients were graphically determined by plotting pressure and density against distance along the tube and drawing a tangent to the curve at the point in question.

Distance from wall. - The zero reading of the probe actuator was found by plotting velocity against distance reading on the probe actuator for a number of runs and extrapolating the curves to zero velocity where all the curves intersected. This extrapolation gave the probe-actuator reading with the probe tip at the wall. The distance of the tip from the wall for each reading could then be easily calculated.

Bulk velocity. - In order to obtain ratios of local to bulk velocity u/u_b at various positions across the tube, the bulk velocity u_b was obtained by plotting u against cross-sectional area πr^2, measuring the area under the curve, and dividing by the total cross-sectional area of the tube πr_0^2. This procedure is equivalent to solving the equation

$$u_b = \frac{\displaystyle\int_0^{\pi r_0^2} u\, d(\pi r^2)}{\pi r_0^2}$$

and gave more accurate values of u/u_b than would have been obtained by use of orifice measurements of weight flow for the determination of u_b, inasmuch as errors in u due to errors in static-pressure measurements were also contained in u_b and any systematic errors tended to cancel.

1323

RESULTS AND DISCUSSION

Variation of Velocity Distribution along Tube

The results of the tests in which variation of the velocity distribution along the tube was determined are summarized in figures 2 and 3. Typical radial velocity distributions at various tube diameters from the rounded entrance of the tube are shown in dimensionless form in figure 2.

In figure 3, which is somewhat more descriptive than figure 2, the variation of velocity along the tube at the center and at $r/r_0 = 0.9$ is shown for both a rounded and a right-angle-edge entrance. The curves show that the development of the velocity distribution was more rapid for the right-angle-edge entrance than for the rounded entrance; with the right-angle-edge entrance fully developed flow was obtained after about 45 tube diameters from the entrance, but with the rounded entrance the distribution was still developing slightly at 100 tube diameters from the entrance. This difference in rate of development was apparently caused by the vena contracta formed at the entrance of the tube with the right-angle-edge entrance, and indicated on figure 3(b) by the points close to the entrance. The presence of the vena contracta accelerated the flow at the center of the tube and thus hastened the development of the distribution.

The curves also show that Reynolds number affected the distribution near the center of the tube because u/u_b decreases as Reynolds number increases. This variation is in agreement with previous findings (reference 6). Difference in Reynolds number has, however, little or no effect on the distribution close to the wall.

A significant observation can be made from figure 3 concerning the difference between the rates of development of velocity distribution at the center of the tube and near the wall. Figure 3 indicates that with both entrances the final distribution is attained much sooner in the vicinity of the wall than at the center of the tube. This fact might explain why, in the present investigation, the static-pressure gradients along the tube caused by friction were only slightly affected by entrance effects. The static-pressure gradient is determined by the velocity gradient at the wall and is unaffected by the distribution in the remainder of the tube.

As will be shown in the discussion of fully developed flow in the section "Effect of Variable Shear Stress," the effect of compressibility on velocity distribution is slight; although some of the determinations were made at high subsonic Mach numbers, it is therefore believed that the results are also applicable to incompressible flow. 1323

Velocity Distributions for Fully Developed Flow

Correlation of experimental data. - The variation of u^+ with y^+ for data obtained near the exit of the test section (that is, for $x/D = 100$) where the flow is fully developed is shown on rectangular coordinates in figure 4(a). The data obtained near the wall are plotted to two y^+ scales. The data are plotted semilogarithmically in figure 4(b). Data for flow close to the wall are shown for only the low flow rates because at high flow rates the severe velocity gradients and the presence of the hole in the tube wall make the accuracy of the measurements doubtful. The data shown were taken with both rounded and right-angle-edge entrances, but the velocity distributions with the two types of entrance were the same within the error of the measurements.

Comparison of the data in figure 4(b) with those of Nikuradse and of Reichardt (reference 3) shows close agreement for all values of y^+ up to about 600. For higher values of y^+, the corresponding values of u^+ are slightly higher than those obtained by Nikuradse (reference 1, p. 242); the maximum deviation, however, is only about 5 percent.

A method of using figure 4 to obtain the velocity distribution for a particular tube when the flow rate is given is indicated in the discussion of figure 8.

Incompressible-flow equations. - The curve corresponding to equation (12) for incompressible flow near the tube wall is included in figure 4 and is in good agreement with the experimental results for values of y^+ from 0 to 26. The value of the constant n in the equation is 0.109, as determined from the experimental data.

An important property of equation (12) is that for small values of y^+, u^+ and y^+ are approximately equal, that is, the flow predicted by the equation is nearly laminar. This approach to equality of u^+ and y^+ is due to the fact that as the wall is approached the eddy diffusivity ϵ becomes very small and is

zero at the wall (equation (5)). The accuracy with which equation (12) predicts the experimental data for y^+ from 0 to 26 obviates the necessity of assuming the existence of a separate layer near the wall that is purely laminar, but does not eliminate the possibility of its existence, as has usually been done in previous investigations. A single equation has therefore been obtained that, for adiabatic incompressible flow, adequately represents the two regions, which are commonly called the laminar layer and the buffer layer. The buffer layer has previously been represented only by empirical equations.

The agreement of equation (12) with the data for values of y^+ from 0 to 26 does not eliminate the possibility of the existence of a very thin layer that is purely laminar, for example, for the region $0 < y^+ < 3$. It is possible that a finite layer exists in which adjacency of the wall completely damps out turbulence. The thickness of the layer then corresponds to some critical wall Reynolds number $\rho u_e y_e/\mu$ where u_e is the velocity at the edge of the layer and y_e is the thickness of the layer. Velocity distributions for $0 < y^+ < 3$ given by equation (12) are practically laminar, however, so that it makes little difference, for calculating velocity distributions, whether the layer is taken into consideration. The only case in which presence of the layer may become important is that of heat transfer in fluids having high Prandtl number, where the turbulence predicted by equation (5), though it may be slight, is important because of the small amount of heat transferred by conduction.

The agreement of equation (12) with the data, together with the discussion preceding the derivation of the equation, indicate that in the region close to the wall the mechanism of turbulent transfer of momentum can be considered affected mainly by quantities that are determined relative to the wall; that is, by the distance of the point from the wall and by the velocity at the point relative to the wall. As was shown in the discussion preceding the derivation of equation (12), the velocity distribution about the point is known to a first approximation when the two quantities u and y are known at the point.

The general form of the equation that is usually employed to represent the turbulent regime was obtained by von Kármán and is, as shown in the analysis section,

$$u^+ = \frac{1}{\kappa} \log_e y^+ + C \tag{15}$$

The values of the constants C and κ, obtained from Nikuradse's data (reference 1), are 5.5 and 0.40, respectively. Corresponding values that represent the present data somewhat better are $C = 3.8$ and $\kappa = 0.36$. The curve representing equation (15) using these values is plotted in figure 4, in which good agreement with the experimental data is indicated for $y^+ = 0$ to $y^+ = 26$. The curves corresponding to the equations for flow near the wall (equation (12)) and flow at a distance from the wall (equation (15)) cross at $y^+ = 26$.

The agreement of equation (15) with the data, together with the discussion preceding the derivation of the equation, indicate that for a region distant from the wall the mechanism of turbulent transfer of momentum can be considered dependent mainly on the flow conditions in the vicinity of the point considered; that is, on the velocities in the vicinity of the point relative to the velocity at the point and not on the position of the point in the tube (the distance from the wall) or on the velocity relative to the wall.

The curves representing equations (12) and (15) have slopes that are not quite equal at their intersection at $y^+ = 26$; this disparity would, however, be expected because the two equations were derived with the assumption that the turbulence mechanism in the two regions is dominated by different factors; hence an abrupt change in turbulence mechanism at the intersection is implied in the equations. Actually, there is probably a gradual change that could not be investigated by the simplified methods used herein. Inasmuch as the actual error in the vicinity of the intersection is insignificant, the present treatment is considered adequate for adiabatic flow.

The value for κ (in equation (15)), which is known as the Kármán constant, was checked by calculating friction factors and Reynolds numbers and plotting $1/\sqrt{4f}$ against $Re\sqrt{4f}$ as shown in figure 5. The line drawn through the data corresponds to the Kármán relation between friction factor and Reynolds number, which is

$$\frac{1}{\sqrt{4f}} = C_2 + \frac{2.303}{\kappa\sqrt{8}} \log \left(Re\sqrt{4f}\right)$$

This equation is derived in reference 2 directly from the equation for velocity distribution. The value of κ was 0.36

as before, and C_2 is found from the data to be - 1.84. Both velocity-distribution and friction-factor data therefore indicate that a value for κ of 0.36 is reasonable, at least for the present tube.

The variation of the ratio of velocity at the center of the tube to bulk velocity with Reynolds number, as indicated in figures 3(a) and (b), can be explained by the plots of the equations in figure 4(a). As y^+ increases the curve becomes flatter. Increasing values of Reynolds number correspond to increasing values of y^+ in the central portion of the tube, so that for high values of Reynolds number the velocity profile in the central portion of the tube becomes flat; thus the ratio of velocity at the center of the tube to bulk velocity becomes less than for low Reynolds numbers.

Effect of variable shear stress. - Neither u^+ nor y^+ are functions of the tube radius. Neglecting the radius in the correlation is equivalent to assuming uniform shear stress across the tube. (See equations (15) and (20) in the section "Analysis.") The results can be correlated by assuming uniform shear stress across the tube because the greatest rate of velocity change with distance from the wall occurs near the wall where the change in shear stress is very small. A comparison between equation (20), which takes into account the variation in shear stress across the tube, and equation (15), which assumes uniform shear stress, is shown in figure 6. The constant C is so determined for each value of r_0^+ that $u^+ = 13$ when $y^+ = 26$. These values were selected in order to make the mean deviation of equation (20) from equation (15) a minimum. The maximum difference between the values of u^+ determined by the two equations is about $2\frac{1}{2}$ percent, which is the same as the scatter of the experimental data points. Equation (15) therefore gives an accuracy comparable to that obtained in most flow measurements so that consideration of the variation in shear stress across the tube does not seem necessary.

Equations for compressible flow. - The equations for compressible flow are presented in figure 7. For graphing equation (29), the value of the integral was found by plotting the integrand against u^+ and planimetering the area under the curve. The constant n was again set equal to 0.109 and d for air was found from viscosity data to have an average value of 0.684 for temperatures between 0° and 2000° F. For plotting equation (33), C_1 was determined for each value of α from the value of u^+ at $y^+ = 26$ found from equation (29). From the definitions of M, $\bar{T}$, u^+,

and α, it can be shown that the relation between u^+, M, γ, and α is

$$u^{+2} = \frac{1}{\alpha\left(\frac{2}{M^2(\gamma-1)} + 1\right)}$$

For $M = 1$, $\gamma = 1.4$, and $\alpha = 0.00025$, u^+ is found to be 25.8. This point is marked on the curve.

As α increases, u^+ decreases for constant values of y^+ (fig. 7). For local Mach numbers up to 1, however, the deviation is slight and, in general, is not more than $2\frac{1}{2}$ percent from the value of u^+ given by the incompressible-flow equation. A single line is used to represent equation (29) because the compressibility effect is so small that it cannot be seen when the equation is plotted to the scale used in this figure.

It therefore appears that with respect to compressibility effects and tube radius or shear-stress variation, the simplified incompressible-flow equations (12) and (15) give an accuracy comparable to that of flow measurements. The fluid properties used in u^+ and y^+ are evaluated at the wall or total temperature.

Flow Rates

The flow rates corresponding to various pressure gradients along the tube can be obtained from the velocity-distribution equations by a graphical integration. For this integration, $(\rho/\rho_0)\ u^+$ was plotted against $(r_0^+ - y^+)^2$, where $\rho/\rho_0 = 1/(1-\alpha u^{+2})$. It can easily be shown that the area under this curve is $w\left(\sqrt{\tau_0/\rho_0}\ \rho_0\right)/\pi g\mu_0^2$. If this dimensionless group is divided by r_0^+ and multiplied by π in order to eliminate τ_0, there results $w/(g\mu_0 r_0)$. This parameter is plotted against r_0^+ for various values of α in figure 8. Figure 8 gives the flow rate to be expected for a given shear stress or friction-pressure gradient. The data of figure 8 also provide a means for obtaining the velocity distribution in a particular tube from the generalized velocity distributions in figures 4 and 7 when the flow rate and the fluid properties are

1323

known. Measured flow rates for conditions where compressibility effects are small are also plotted in figure 8 and agree closely with the curve for $\alpha=0$. The curves indicate that at a Mach number of 1, compressibility effects increase the flow-rate parameter $w/(g\mu_0 r_0)$ by about 12 percent. Several data points corresponding to higher values of α are also plotted in the figure and the trends corresponding to increasing values of α appear to be similar to the predicted trends, although no definite conclusion can be drawn from the limited range of values of α shown. Data corresponding to higher values of α are not plotted because reliable measurements of the severe pressure gradients involved could not be obtained.

CONCLUDING REMARKS

The results obtained in this investigation should be applicable to any gas to which the perfect gas law applies and for which the Prandtl number is close to 1. The value of the exponent d for viscosity variation with temperature was obtained specifically for air, but it occurs only in the equation for compressible flow close to the wall where compressibility effects are negligible. The equations and the curves for incompressible flow should, of course, also be applicable to liquids, inasmuch as the fluid properties that determine the flow phenomena are common to liquids and gases.

SUMMARY OF RESULTS

The following results were obtained from the analytical and experimental investigation of the adiabatic flow of air through a smooth tube having an inside diameter of 0.87 inch and a length of 87 inches:

1. The length of tube required for obtaining fully developed flow was greater with a rounded entrance than with a right-angle-edge entrance. With a rounded entrance, the flow at the axis of the tube was still developing slightly at 100 diameters from the entrance. For both entrances, however, the flow close to the wall developed in a much shorter distance than did the flow in the center of the tube. The flow close to the wall determines the shear stress or pressure gradient along the tube, so that the effect of entrance on these factors is slight except for very short tubes.

2. A good correlation of velocity-distribution data for fully developed flow was obtained by using the well-known dimensionless velocity and distance parameters. The data agreed closely with those of Nikuradse and other investigators. 1323

3. The equation derived for adiabatic incompressible flow close to a wall represented well the relation between the velocity and distance parameters found experimentally for the two regions that have generally been called the laminar layer and the buffer layer.

4. The analysis and experimental investigations indicated that the effect of variable shear stress on velocity distributions is slight; the maximum variation in the velocity parameter caused by this effect was approximately $2\frac{1}{2}$ percent.

5. The compressible-flow equations showed that the effects of compressibility on velocity distributions are small for Mach numbers up to 1; the maximum variation in the velocity parameter caused by compressibility effects was approximately $2\frac{1}{2}$ percent.

6. The simplified incompressible-flow equations derived on the assumption of uniformity of shear stress across the tube predicted velocity distributions in smooth tubes for Mach numbers up to 1 with an accuracy comparable to that of flow and pressure measurements.

7. Graphical integration of the velocity-distribution equations gave flow rates that agreed closely with flow rates from orifice measurements.

Lewis Flight Propulsion Laboratory,
National Advisory Committee for Aeronautics,
Cleveland, Ohio, January 9, 1950.

1323

APPENDIX - SYMBOLS

The following symbols are used in the report:

A	internal cross-sectional area of tube, sq ft
C,C_1,C_2	constants of integration
c_p	specific heat of fluid at constant pressure, Btu/(lb)(°F)
D	inside diameter of tube, ft
d	exponent that describes variation of viscosity of fluid with temperature
g	acceleration due to gravity, 32.2 ft/sec^2
J	mechanical equivalent of heat, 778 ft-lb/Btu
n	constant
P	total pressure, lb/sq ft absolute
p	static pressure, lb/sq ft absolute
R	perfect gas constant, ft-lb/(lb)(°R)
r	radius, distance from tube center, ft
r_0	inside tube radius, ft
T	total temperature, °R
T_0	absolute wall total temperature, °R
t	absolute static temperature, °R
t_b	bulk or average static temperature of fluid at cross section of tube, °R
u	velocity parallel to axis of tube, ft/sec
u_b	bulk or average velocity at cross section of tube, ft/sec
u_c	velocity at center of tube, ft/sec

w fluid-flow rate, lb/sec

x axial distance from tube entrance, ft

y distance from tube wall, ft 1323

γ ratio of specific heat at constant pressure to specific heat at constant volume

ϵ coefficient of eddy diffusivity, sq ft/sec

κ Kármán constant

μ absolute viscosity of fluid, lb-sec/sq ft

μ_0 absolute viscosity of fluid at wall, lb-sec/sq ft

ρ mass density, lb-sec^2/ft^4

ρ_b bulk or average density at cross section of tube, lb-sec^2/ft^4

ρ_0 mass density of fluid at wall, lb-sec^2/ft^4

τ shear stress in fluid, lb/sq ft

τ_t shear stress produced by turbulence, lb/sq ft

τ_v shear stress produced by viscosity, lb/sq ft

τ_0 shear stress in fluid at wall, lb/sq ft

Subscripts:

fr on friction pressure gradient

mom on momentum pressure gradient

Dimensionless parameters:

α compressibility parameter, $\dfrac{\tau_0}{2gJc_pT_0\rho_0}$

f friction factor, $-\dfrac{D\left(\dfrac{dp}{dx}\right)_{fr}}{2\rho_b u_b^2}$

M Mach number, $\dfrac{u}{\sqrt{\gamma g R t}}$

Re Reynolds number, $\dfrac{\rho_b u_b D}{\mu_0}$

r_0^+ tube-radius parameter, $\dfrac{\sqrt{\tau_0/\rho_0}}{\mu_0/\rho_0} r_0$

u^+ velocity parameter, $\dfrac{u}{\sqrt{\tau_0/\rho_0}}$

y^+ wall-distance parameter, $\dfrac{\sqrt{\tau_0/\rho_0}}{\mu_0/\rho_0} y$

REFERENCES

1. Rouse, Hunter: Fluid Mechanics for Hydraulic Engineers. McGraw-Hill Book Co., Inc., 1938.

2. von Kármán, Th.: Turbulence and Skin Friction. Jour. Aero. Sci., vol. 1, no. 1, Jan. 1934, pp. 1-20.

3. Reichardt, H.: Heat Transfer through Turbulent Friction Layers. NACA TM 1047, 1943.

4. Rosenbach, Joseph B., Whitman, Edwin A., and Moskovitz, David: Mathematical Tables. Ginn and Co., 1937, pp. 186-187.

5. Bakhmeteff, Boris A.: The Mechanics of Turbulent Flow. Princeton Univ. Press, 1941, p. 2.

6. Prandtl, L., and Tietjens, O. G.: Applied Hydro- and Aeromechanics. McGraw-Hill Book Co., Inc., 1934, p. 48.

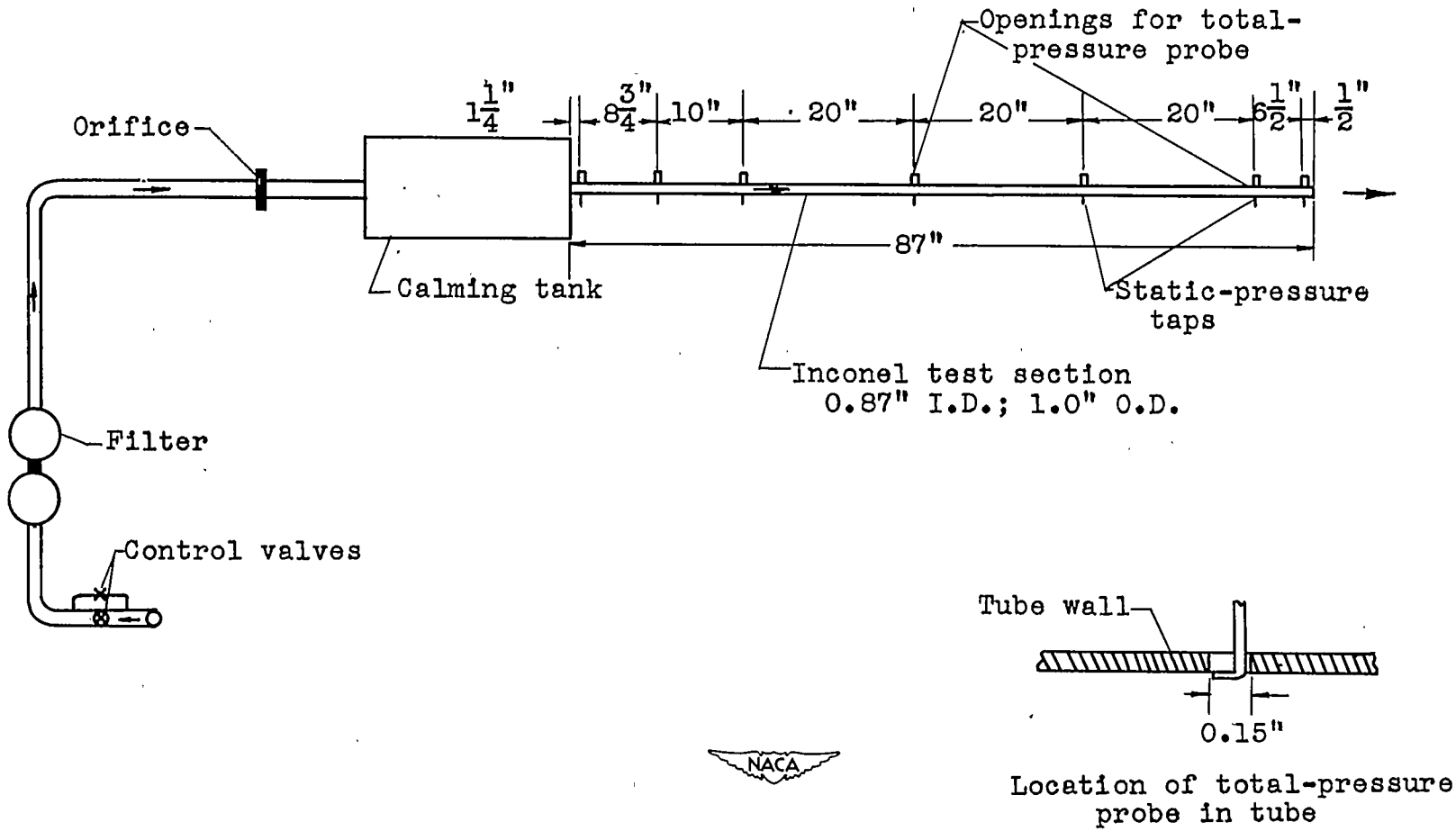

Figure 1. - Apparatus for measuring velocity distributions.

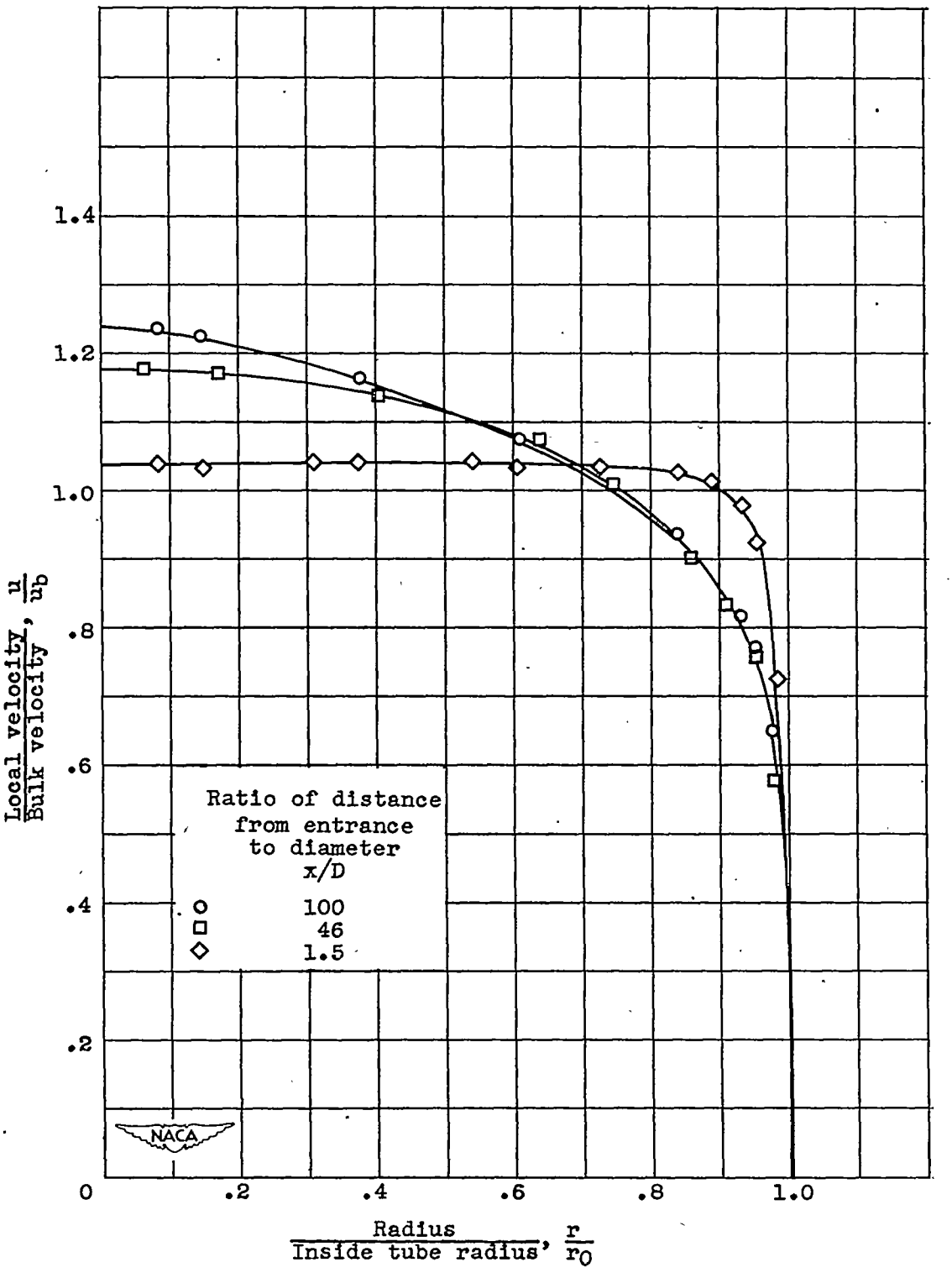

Figure 2. - Typical velocity distributions for flow through tube with rounded entrance at various distances from entrance. Reynolds number, 46,000.

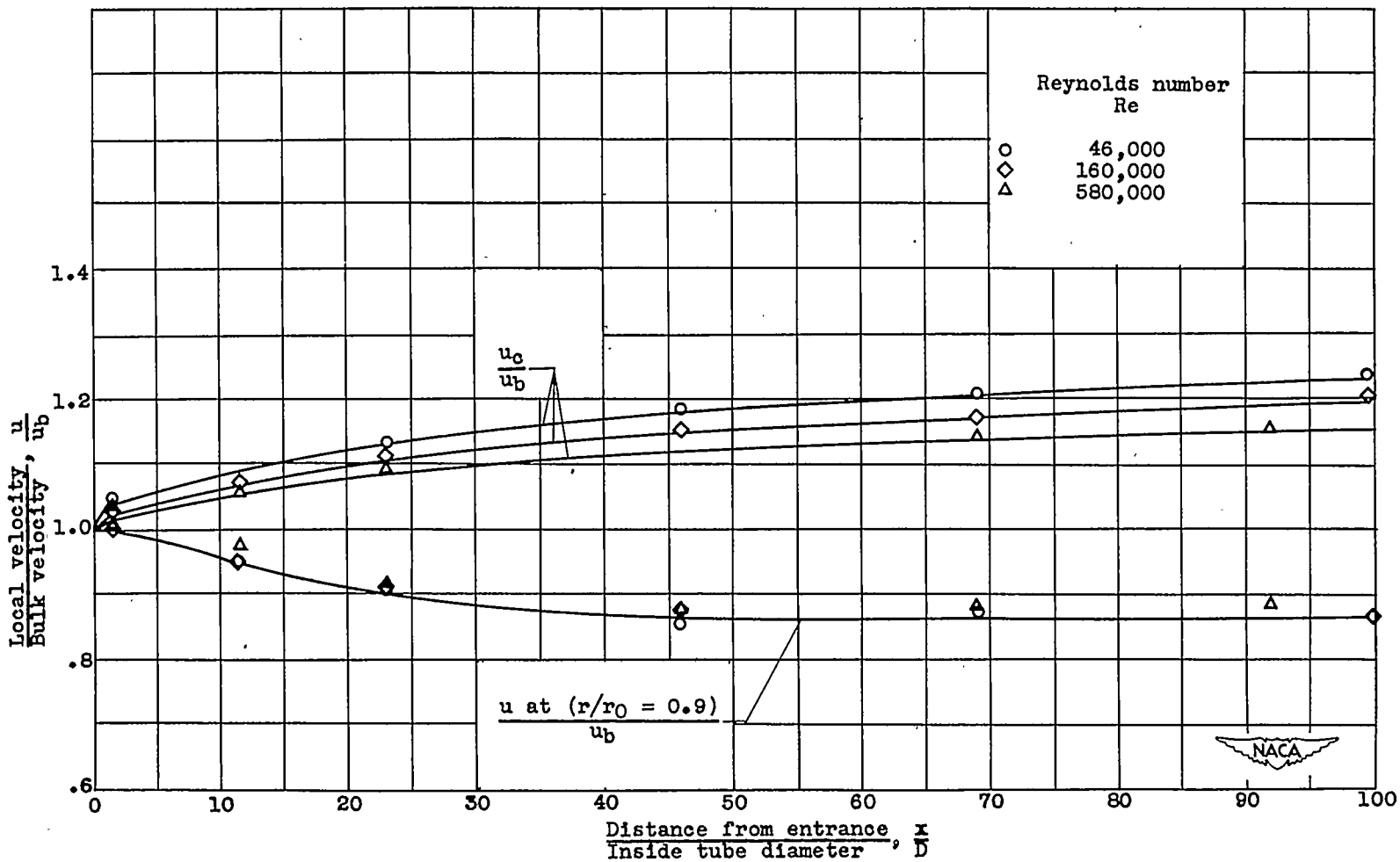

(a) Rounded entrance.

Figure 3. - Development of velocity distributions for flow through tube.

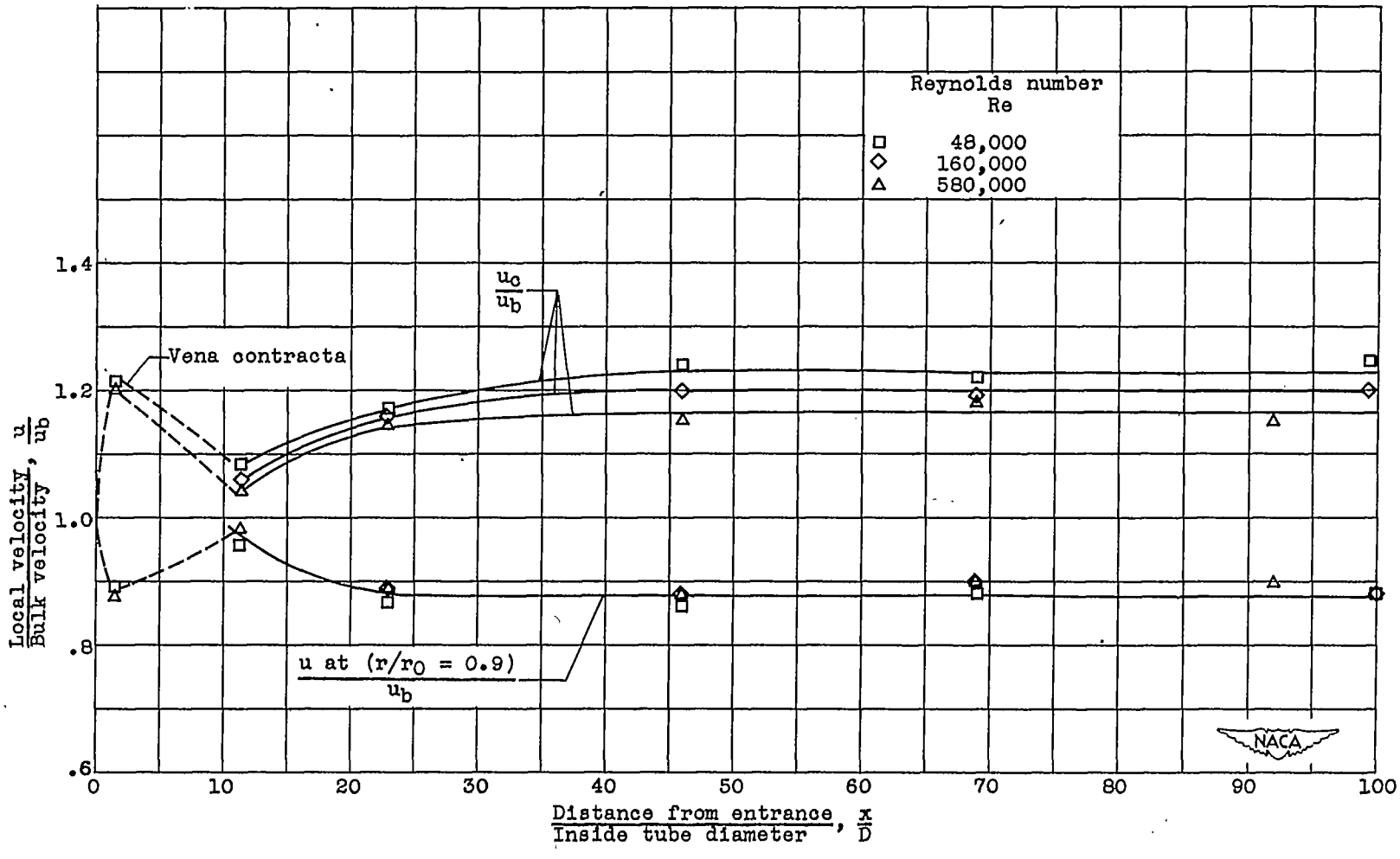

(b) Right-angle-edge entrance.

Figure 3. - Concluded. Development of velocity distributions for flow through tube.

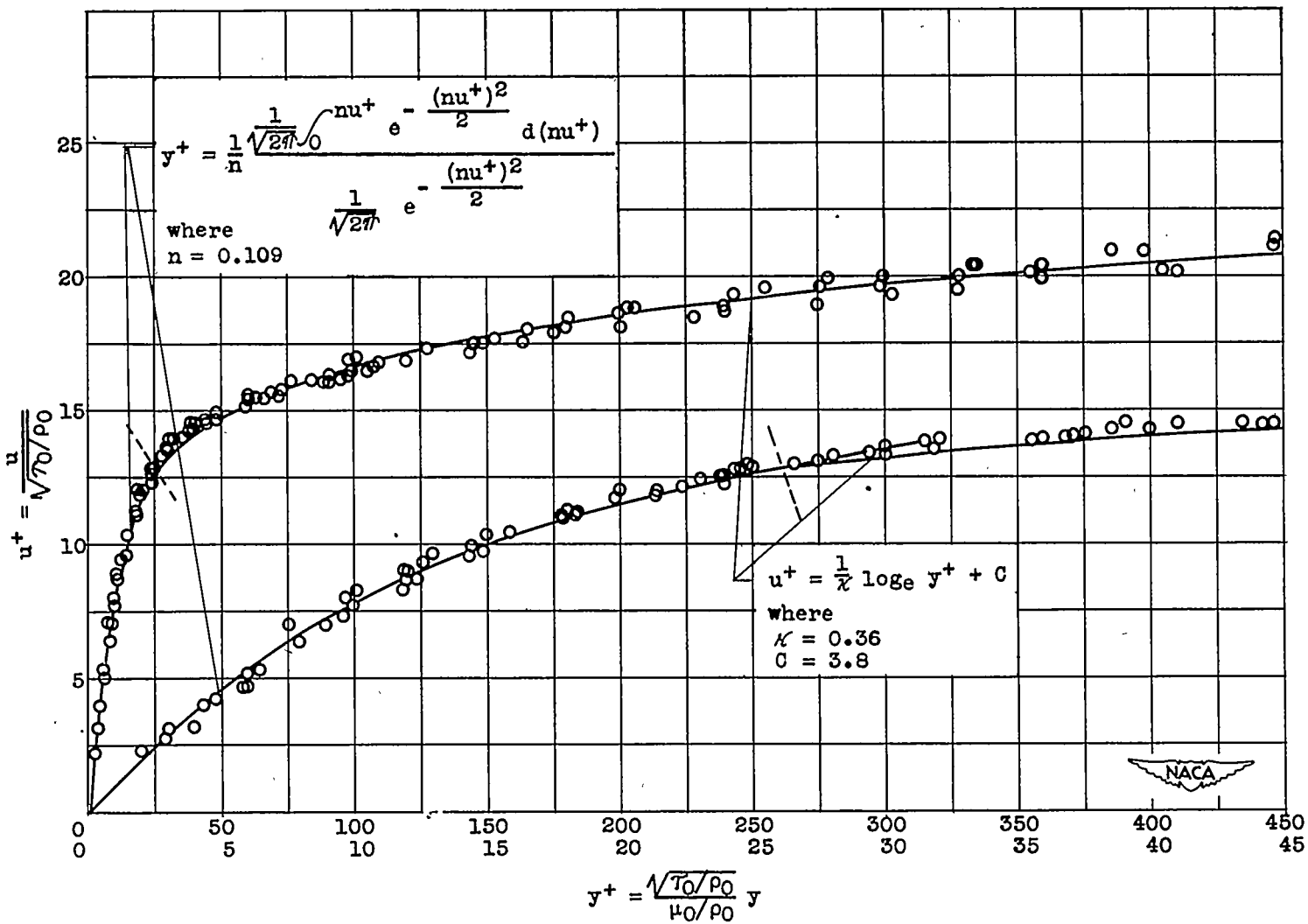

(a) Rectangular coordinate plots with data obtained near the wall plotted to two y^+ scales.

Figure 4. - Generalized velocity distribution for fully developed flow in smooth tubes.

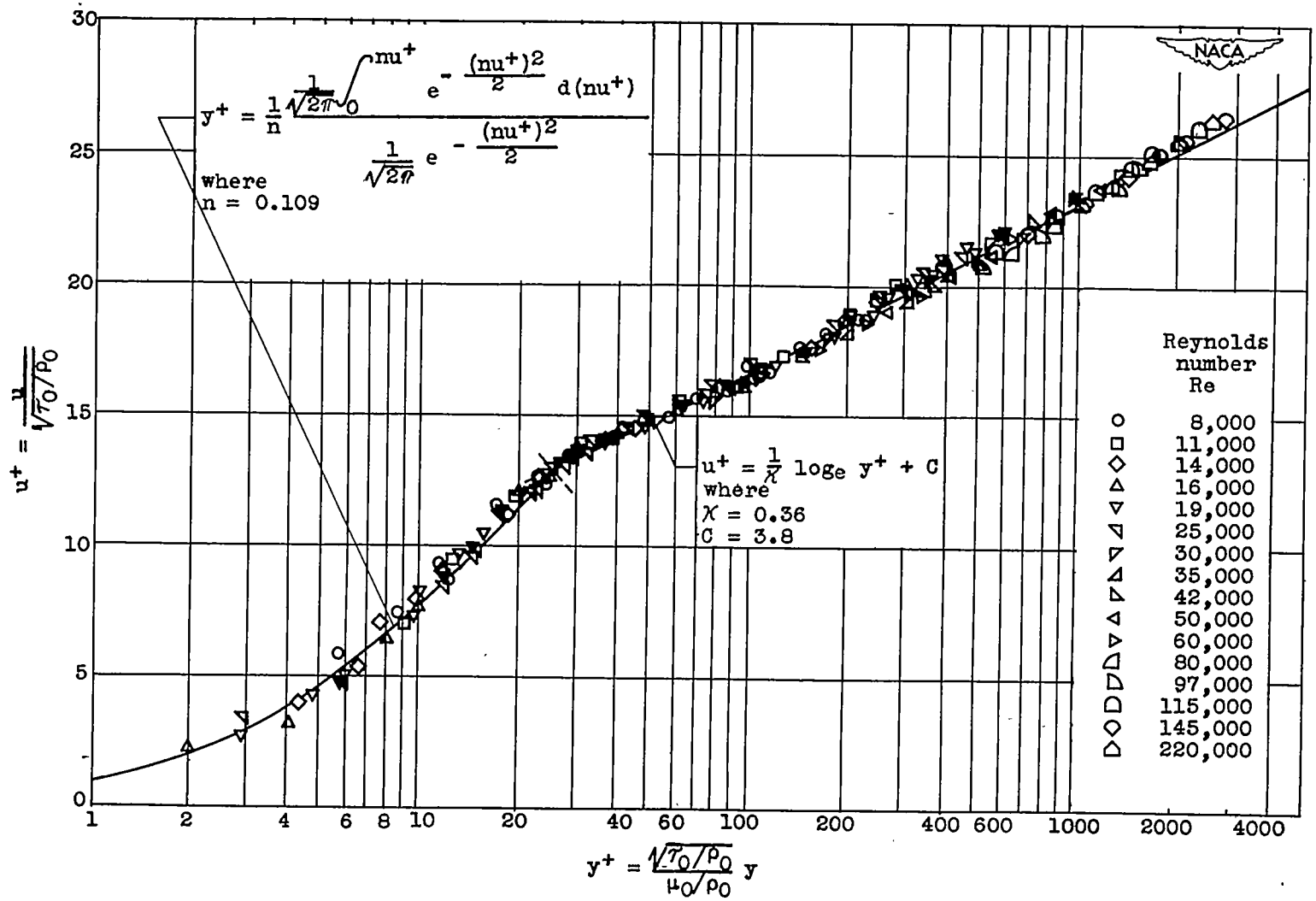

(b) Semilogarithmic plot.

Figure 4. - Concluded. Generalized velocity distribution for fully developed flow in smooth tubes.

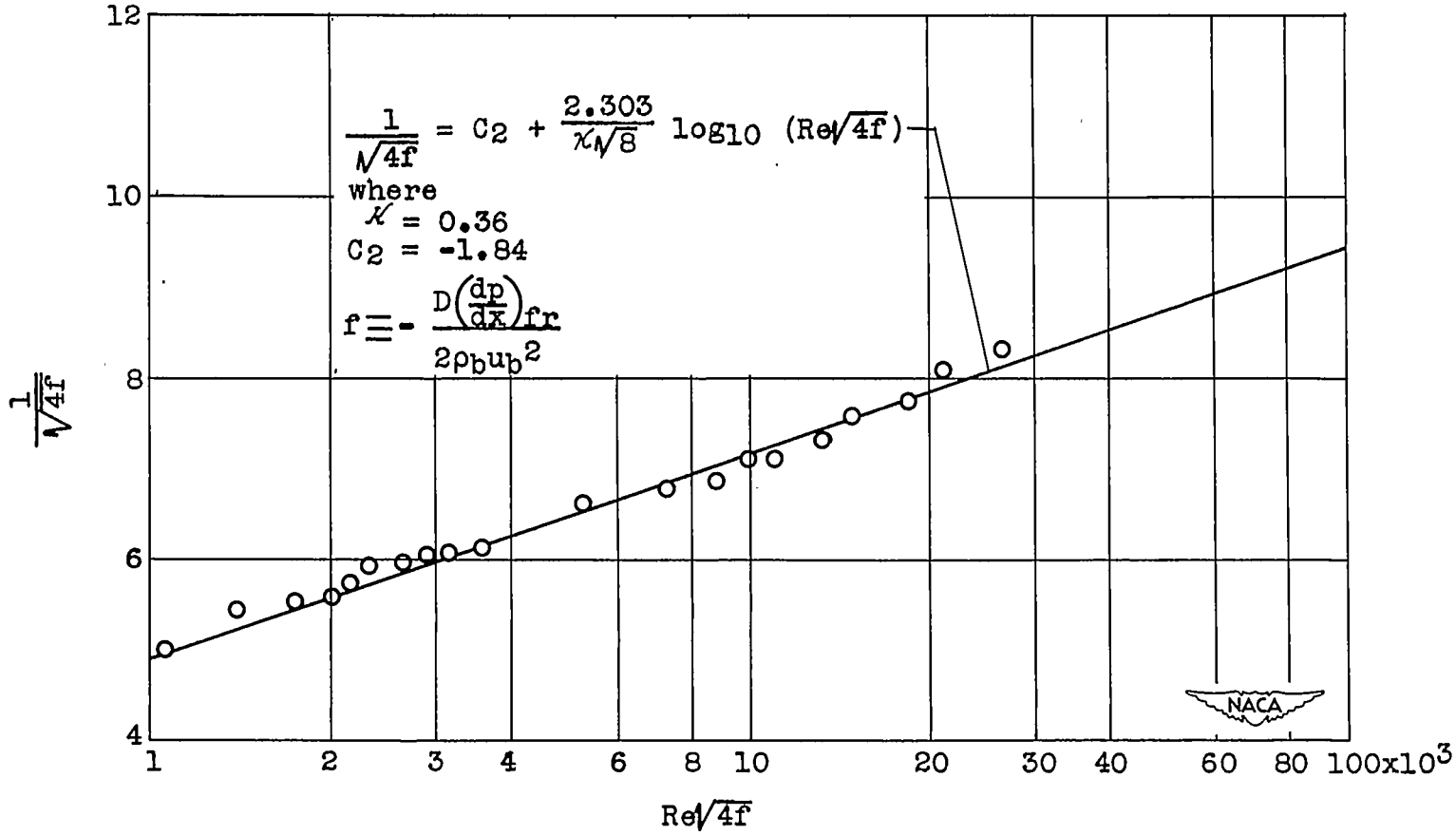

Figure 5. - Determination of the Karman constant $\varkappa$ from friction-factor data.

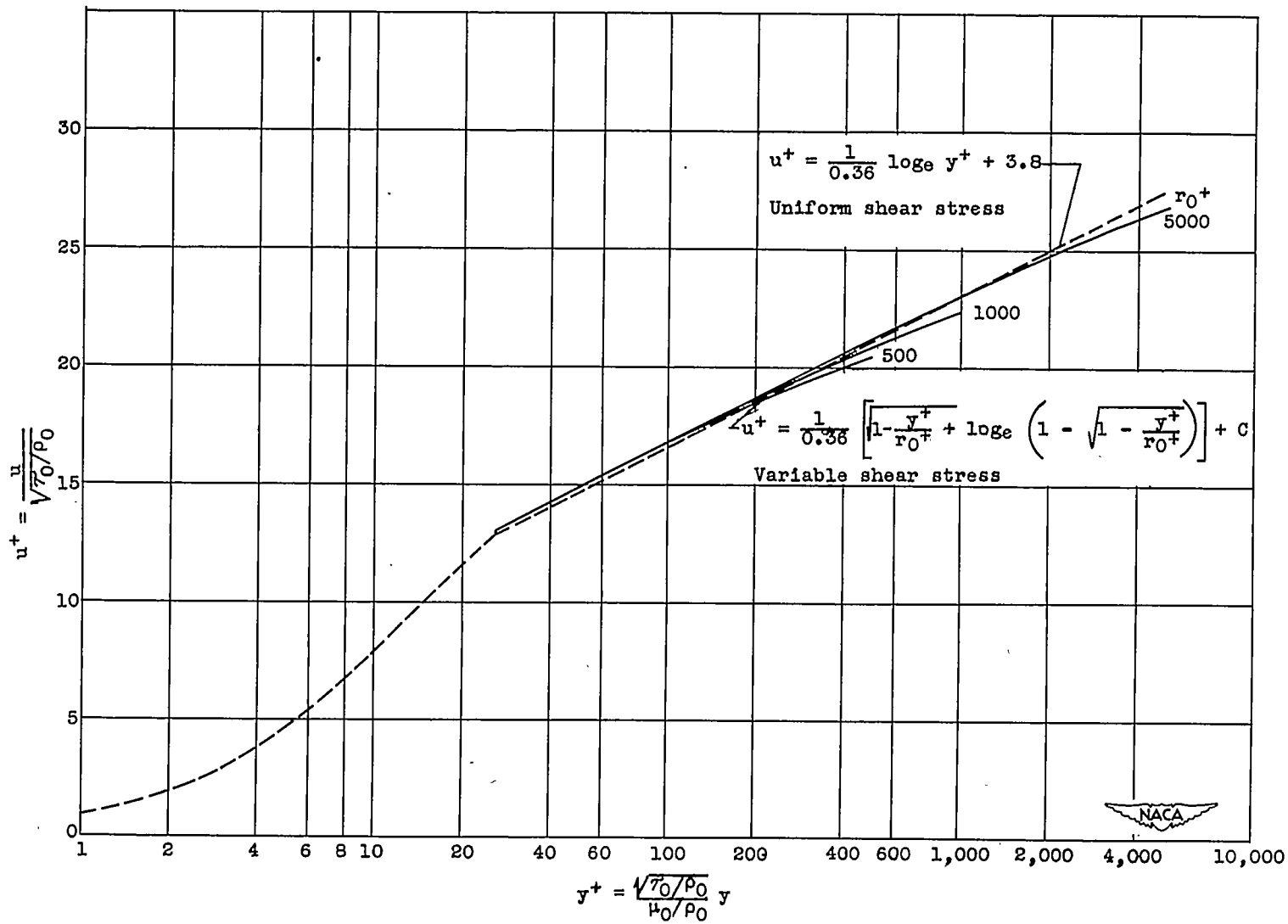

Figure 6. - Comparison of equation derived by assumption of uniform shear stress with equation accounting for variation of shear stress across tube.

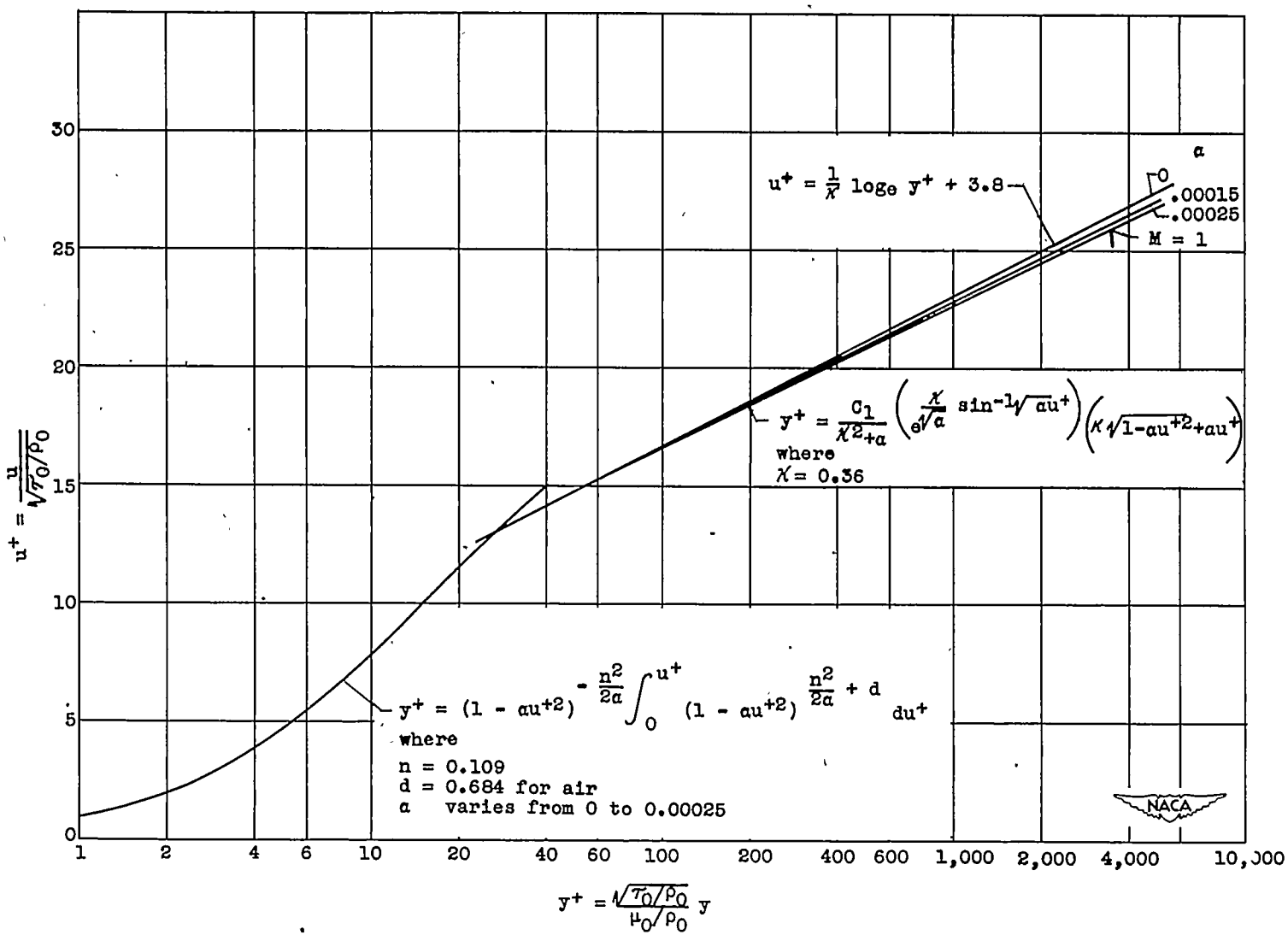

Figure 7. - Velocity-distribution equations for compressible flow in smooth tubes.

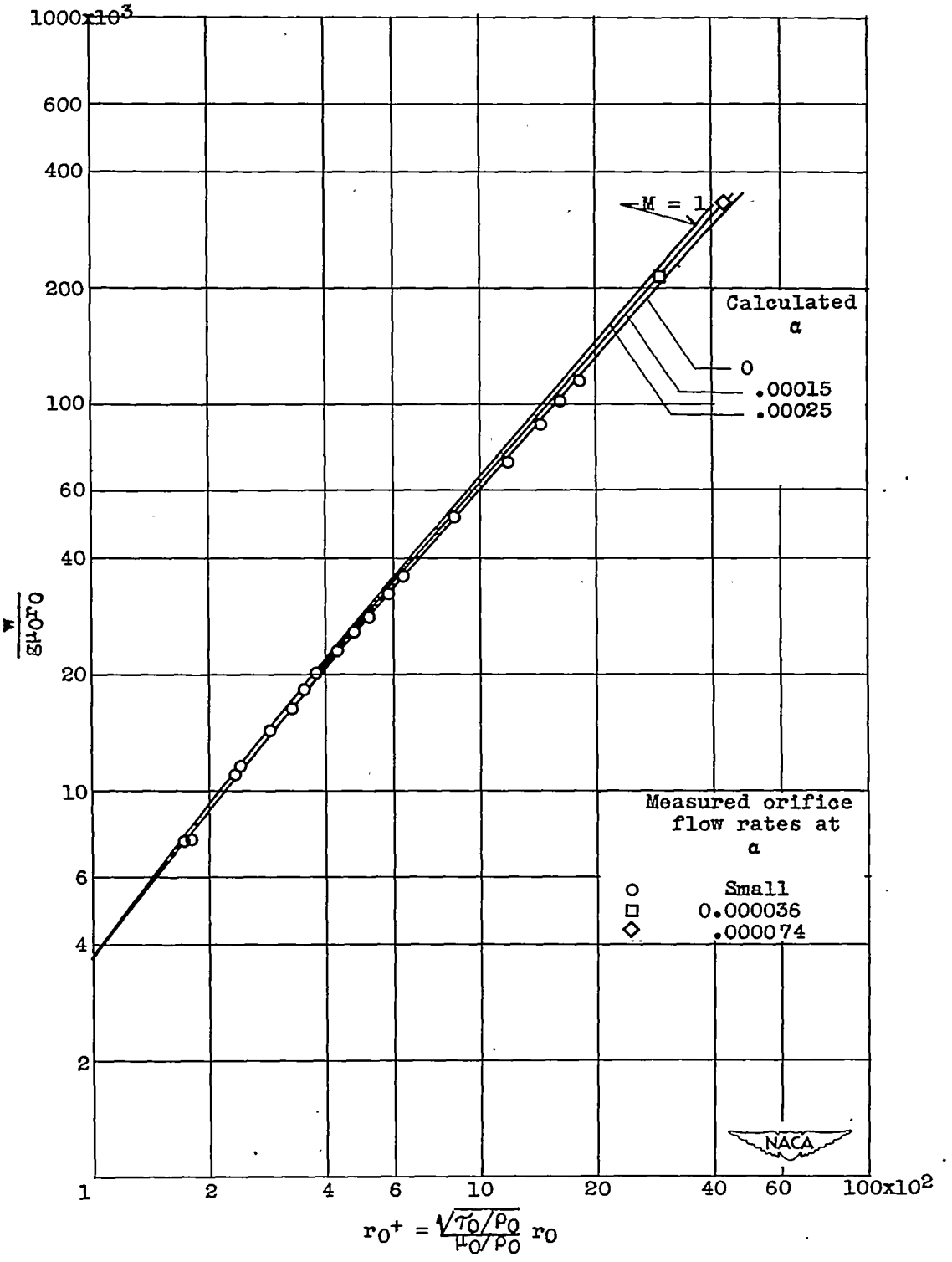

Figure 8. - Variation of dimensionless flow-rate parameter obtained by graphical integration of velocity-distribution equations with tube-radius parameter.

NACA-Langley - 7-19-50 - 1100